metals

MDPI

Article

A Numerical Study on Contact Condition and Wear of Roller in Cold Rolling

Qichao Jin [1], Wenhu Wang [1], Ruisong Jiang [1], Louis Ngai Sum Chiu [2,3], Di Liu [4] and Wenyi Yan [2,*]

1 The Key Laboratory of Contemporary Design and Integrated Manufacturing Technology, Ministry of Education, Northwestern Polytechnical University, Xi'an 710072, China; jinqichao999@mail.nwpu.edu.cn (Q.J.); npuwwh@nwpu.edu.cn (W.W.); jiangrs@nwpu.edu.cn (R.J.)
2 Department of Mechanical & Aerospace Engineering, Monash University, Clayton, VIC 3800, Australia; louis.ngai.chiu@monash.edu
3 Institute for Frontier Materials, Deakin University, Waurn Ponds, Geelong, VIC 3216, Australia
4 National Key Laboratory for Precision Hot Processing of Metals, Harbin Institute of Technology, Harbin 150001, China; liudi_hit@126.com
* Correspondence: wenyi.yan@monash.edu; Tel.: +61-04-3224-6278

Received: 7 July 2017; Accepted: 11 September 2017; Published: 15 September 2017

Abstract: An accurate determination of the contact pressure and local sliding in a cold rolling process is an essential step towards the prediction of the roller's life due to wear damage. This investigation utilized finite element analysis to quantify the local contact pressure and local sliding over the rolling bite in a plate cold rolling process. It was the first study to quantify the local sliding distance in a rolling process using the Finite Element Analysis (FEA). The numerical results indicate that the local contact pressure over the rolling bite demonstrates a hill profile, and the peak coincides with the neutral plane. The local sliding distance over the rolling bite demonstrates a double-peak profile with the two peaks appearing at the forward slip and backward slip zones respectively. The amplitude of sliding distance in the backward slip zone is larger than that in the forward slip zone. A stick zone was confirmed between the forward slip and backward slip zones. According to a parametric study, the local contact pressure and sliding distance decrease when the thickness reduction is reduced or the diameter of the roller is decreased. The location of the neutral plane always presents at the rolling exit side of the rolling bite's center. The size of the stick zone enlarges and the sizes of slip zones shrink significantly when the friction coefficient is increased. Finally, a novel concept of wear intensity was defined to examine the wear of the roller based on the local contact pressure and local sliding distance. The results show that a two-peak wear response exists in the backward and forward slip zones. The magnitude of the wear in the backward slip zone is larger than that in the forward slip zone. For a given roller and blank material combination, using a smaller thickness reduction, a smaller diameter roller and a higher friction coefficient condition can reduce the wear of the roller for a single rolling cycle. The current paper develops an understanding of rolling contact responses to the wear of the roller in rolling process. The research method can also be applied to study other rolling or sliding wear problems.

Keywords: cold rolling; contact pressure; local sliding distance; wear; finite element

1. Introduction

Metal rolling is a form of continuous casting process. A large majority of metal products, such as plates, beams, rails and blades, are produced by rolling [1]. The cold rolling process has high manufacturing efficiency and produces a component with good in-service performance due to work hardening. The roller needs to withstand high periodic forming forces for extended periods of time,

and the rolling contact causes an unacceptable level of wear on the roller [2]. Wear can be costly due to the need for expensive wear-resistant materials and coatings. Wear of the roller also increases the need for stoppage and maintenance, and leads to poor finished surface quality and reduced geometric accuracy. Consequently, the study of wear and the life prediction of the roller become increasingly necessary.

Wear is a natural consequence of friction. It is the progressive loss of material from the surface of a body as a result of relative motion at the surface [3]. It is a function of contact condition such as normal load, relative displacement amplitude and frequency [4]. Wear can be studied via the empirical equations, the contact mechanics approach or the failure mechanics approach [5]. Wear is a complex interaction between material properties and mechanical action. Pereira et al. [6–8] investigated the contact pressure and local sliding over the die radius in a stamping process, and the possible trends of wear over the radius were predicted. Szota et al. [9] presented a methodology for quantifying wear of rollers based on simulation results for a round bar rolling processes. Mattei and Puccio [10] proposed a generalization of the Archard wear model to study the wear of a cylinder sliding over a plane with different stroke amplitudes, and calculated the evolution of wear volumes, wear profiles and contact variables with travelled distance. Following Archard's wear model [11], for a given material combination and contact surface condition, both abrasive and adhesive wear at a local area depend on the local contact loading conditions, which can be described by the local contact pressure P, and the relative local sliding distance S. Generally, this relationship can be described by [6–8,12].

$$w = kP^m S^n \tag{1}$$

where w represents the local wear intensity, that is, wear volume per unit area over the sliding distance S; k is the wear coefficient which depend on the contact surface conditions, such as surface roughness, and the materials properties including the hardness of the materials; m and n are the exponent coefficients for contact pressure P and sliding distance S, respectively. Hence, understanding the rolling contact condition is a vital step for studying wear. The local contact pressure and localized sliding depends on the shape, the material and the relative motion of the contact pairs. For a rolling process, the contact response is complex because the blank is an elastic-plastic part, and the roller is an elastic part if ignoring the small plastic deformation. The slab method is essential way for analyzing the contact and deformation of rolling process [13–15]. It is generally believed that the rolling bite, that is, the rolling contact area, can be divided into the forward slip zone and backward slip zone, as illustrated in Figure 1. The roller's local tangential speed is smaller than the local speed of the blank in the forward slip zone, which is opposite in the backward slip zone. Dong and Song [16] studied the slip in bar rolling and found that the difference between the roller's and blank's speeds induces local sliding. Kazeminezhad and Taheri [17] analyzed the contact pressure in wire flat rolling, the local contact pressure distributed as a hill with the peak occurring at the neutral plane. The local sliding and normal load cause local wear of the roller.

This paper studies the wear characteristics of the roller based on the numerically obtained local contact pressure and local sliding. An FEA model was set up for the rolling process. An arithmetic method was used for calculating the local sliding distance over the rolling bite. The distributions of the contact pressure and local sliding distance of roller were analyzed, and the major rolling parameters were investigated. The wear of the roller was examined based on the numerical contact pressure and the local sliding distance. The investigation of wear behavior over the rolling bite for rolling process was carried out.

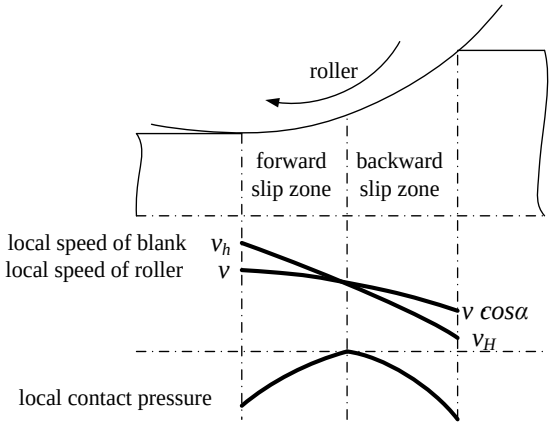

Figure 1. Illustration of the sliding and the contact pressure in the forward and backward slip zones at the rolling bite.

2. Research Methods

2.1. Outline for Studying Contact Reponses and Wear of Roller

This paper used finite element analysis to study the local contact responses and wear of roller in a symmetric rolling process. The flowchart of the study is showed in Figure 2. Firstly, an FEA model was established and validated for a plate rolling process. Secondly, the local contact pressure and local sliding distance over rolling bite were obtained based on numerical results, and the effects of rolling parameters were investigated. Thirdly, the local nominal wear of rolling bite and total wear over the roller were studied based on the wear Equation (1). Finally, the nominal wear distribution over rolling bite and the total wear of roller were investigated.

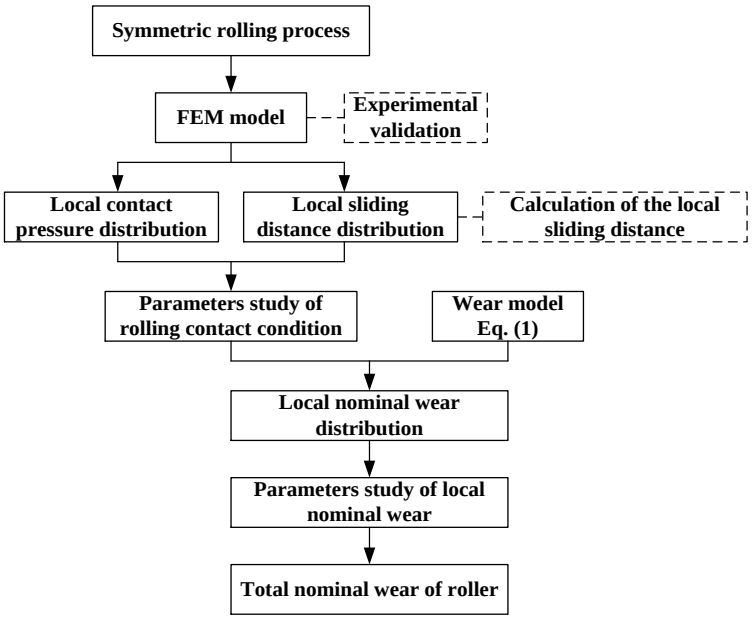

Figure 2. Flowchart for studying the local contact responses and wear of a roller in cold rolling.

2.2. Finite Element Model

In order to determine the contact response in the rolling process, a FEA simulation is used in this paper. A typical rolling process is shown in Figure 3a. The process variables are summarized in Table 1.

The chosen process parameters are typical for a plate rolling process. The material of the blank is magnesium alloy (AZ31). The material of roller is A532M, which is a typical steel for cold-forming die with good wear resistance. The isotropic material properties of the blank and roller are summarized in Table 2, and the plastic property of blank is shown in Figure 4. The rolling process was replicated in the numerical simulation using a non-linear implicit FEA code (ABAQUS/Standard Version 6.14-1, SIMULIA, Providence, RI, USA). The classical von Mises plasticity model was used to describe the plastic deformation of the plate in the simulations. The analysis was simplified to a one-half symmetry, two-dimensional plane strain problem. In order to analyze the contact responses of the roller in detail, the roller mesh and blank mesh were significantly refined in the region of respective interfaces as shown in Figure 3b. The four-node, bilinear, plane strain, quadrilateral, reduced integration elements with enhanced hourglass control (CPE4R) were used to mesh the roller and blank. The Coulomb friction model was used between roller and blank. Convergence check was carried out to ensure that the mesh is fine enough to have converged results, as shown in Figure 5. This figure clearly indicates both the peak contact pressure and the maximum sliding distance converged to constant values with the reduction of the mesh size in the contact area. Consequently, the fine mesh size of model was 0.05 mm in the investigation. The von Mises stress in a rolling process is shown in Figure 3c.

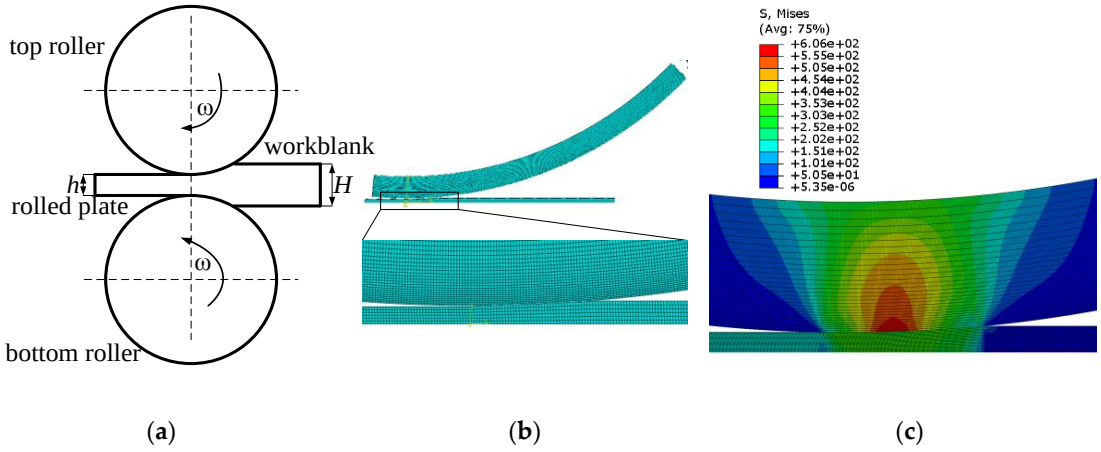

Figure 3. Rolling process and finite element model for simulation. (**a**) Schematic of a plate rolling process, (**b**) simplified Finite Element Analysis (FEA) model of the rolling process, (**c**) von Mises stress from a rolling process simulation.

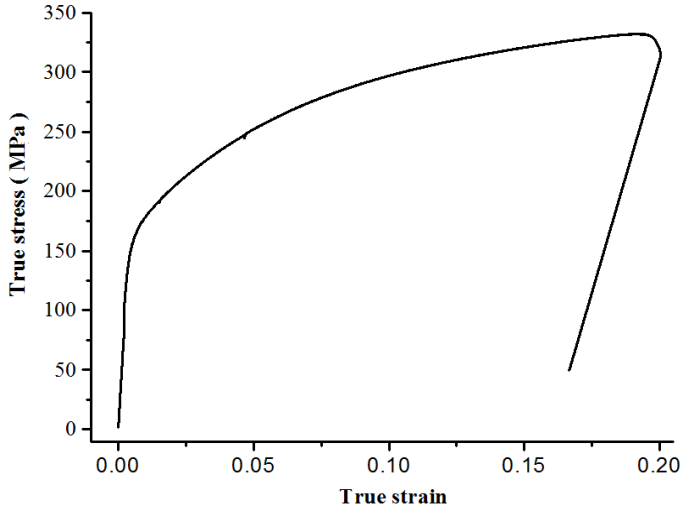

Figure 4. The stress-strain curve of AZ31 under uniaxial tension.

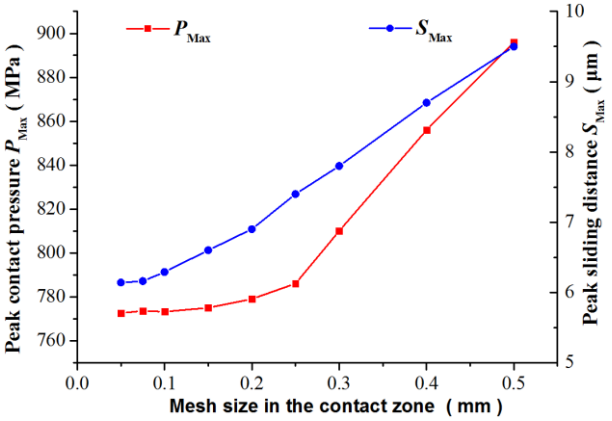

Figure 5. Mesh convergence check for both peak contact pressure and peak sliding distance over the rolling bite.

Table 1. Summary of process parameters for the rolling process simulation.

Parameter	Symbol	Value
Plate Thickness	h	1.5 mm
Thickness reduction	ε	25%
Radius of roller	r	95 mm
Friction coefficient	μ	0.25
Angular velocity	ω	0.35 rad/s

Table 2. Material properties of blank and roller.

Material Properties	Blank	Roller
Material behavior	Elastic-plastic	Elastic
Density (kg/m^3)	1780	7850
Young's modulus (GPa)	37.4	215.6
Poisson's Ratio	0.3	0.3

2.3. Calculation of Local Sliding Distance

According to Equation (1), the local contact pressure and sliding distance are two important parameters for wear estimation. The sliding displacement begins to accumulate from the entrance section to the exit section. In order to calculate the wear of the roller, the sliding distance of each roller surface node over rolling bite must be determined. However, the simulation result only provides the accumulated sliding displacement in contact surface. Pereira et al. [7] provided a method for calculating the sliding distance with the variation of time-increment. In the plate rolling process, the rolling parameters and the geometrical parameters of rollers and blank are unchanged. Hence, the shape of the rolling bite keeps a steady state, and local contact condition over rolling bite remains unchanged, which can be referred to calculate the local sliding distance with the variation of node number in the steady-state rolling process, as shown in Figure 6. In a rolling cycle, an arbitrary material point A on the roller surface experiences the sliding against the plate surface, which causes wear at point A. The local sliding distance S^A, in a short way S, of the material point A can be calculated based on the difference of the accumulated relative sliding distances x_i^A to x_{i+1}^A against the contacting plate surface when it moves corresponding to finite element node i to the next location of the finite element node $i+1$ within the time increment of Δt in a steady state rolling process. If the angular velocity is ω and the angular distance between nodes $i+1$ and i is $\Delta\alpha$, the time increment is $\Delta t = \frac{\Delta\alpha}{\omega}$. If the local contact pressure $P^A = 0$, the local sliding distance $S_i^A = 0$; otherwise the local contact pressure should be $P^A > 0$, and the local sliding distance $S_i^A = x_{i+1}^A - x_i^A$. To ensure the consistence of the time increment for calculating the local sliding distance for all the material points on the roller, uniform element size

on the contact surfaces in the finite element model is required. Additionally, considering the numerical floating error in a computational simulation, the local sliding distance is treated as zero if a calculated local sliding distance is less than is 0.05 μm, which is one-thousandth of the mesh size on the rolling bite. This treatment is also necessary to clearly define a stick zone as discussed in next section.

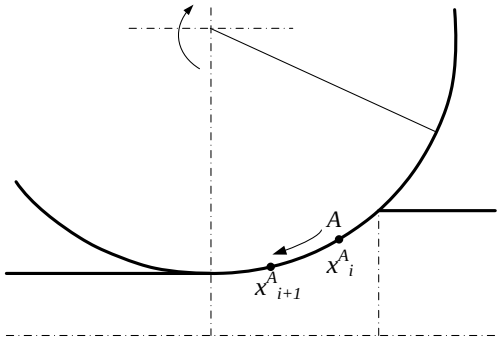

Figure 6. Schematic for calculating the local sliding distance from an FEA simulation.

3. Numerical Results

Analyzing the local contact pressure and sliding is an effective method to understand the contact response of the roller. This section presents the analysis of contact pressure and sliding over the rolling bite. Meanwhile, the rolling parameters were investigated to have a better understanding of the rolling contact condition.

3.1. Distribution of Local Contact Pressure and Local Sliding Distance

Dong et al. [18] studied the contact responses using partial slip contact model, and a semi-analytic method was used to investigate the pressure, tangential tractions, plastic zones and subsurface stress fields among the contact bodies. The contact pressure and sliding in a pair of structures in a relative motion are complex and time- and location-dependent. During the steady-state rolling process, the shape of the rolling bite remains unchanged and the distribution of the contact pressure and sliding over the rolling bite also remain constant. The simulated contact responses are shown in Figure 7. The local contact pressure has a hill-shaped distribution over the rolling bite, as shown in Figure 7a. Kazeminezhad and Taheri [17] termed it as a "friction hill" in their study of the rolling contact condition in a wire rolling process. The largest contact pressure occurred at the neutral point with the magnitude of 772.6 MPa and the neutral angle was 1.83°, as shown in Figure 7a. Weisz-Patrault et al. [19] defined the neutral point as the position where the largest contact pressure occurs over the rolling bite. Its location can be expressed by an angular coordinate value with the origin from the initial contact point on the rolling bite. The relative location of the neutral point is specified as the percentage of its angular coordinate along the rolling bite. If the neutral point location is α_n, the angular size of the rolling bite circular arc is α_C, the relative location of the neutral point is α_n/α_C. The neutral point is an important feature of a rolling process, because it is a distinct boundary for distinguishing the direction of sliding and shear stress. Typically, the neutral point is in the center of the region of zero shear stress within the surface formed by the interface between the two parts. The local contact pressure begins to increase at the entrance section and achieves peak value at the neutral point, and it starts to decrease from the neutral point to the exit section, as shown in Figure 7a. The neutral point becomes the boundary separating the loading and unloading process within the rolling bite. Dong et al. [20] have obtained the neutral point of the rolling contact surface by solving the velocity of flow. The rolling bite can be divided into three parts along the rolling direction based on simulated sliding displacement, that is, the backward slip zone, the stick zone and the forward slip zone, which are shown in Figure 7b. Jiang et al. [21] calculated the frictional shear stress in a rolling process and also obtained a stick zone and two slip zones based on the distribution of the shear stress. The local sliding distance from our

numerical results distributes as a double peak curve, and the peak value of the backward slip zone is bigger than that of the forward slip zone. The sliding speed distributes as a step-curve, and two partial peaks express at the backward and forward slip zone with inverse direction. This type of sliding contact response was found between other contact interfaces [22]. The contact response begins at the backward slip zone and ends at the forward slip zone along the rolling direction. The backward slip zone spans from 4.16° to 2.63°. The roller surface begins to contact with the blank at 4.16° and the points on the surface of the roller is sliding towards the neutral point. With decreasing contact angle, the local sliding distance decreases from 6.14 to 0 μm, and the local sliding speed decreases from 4.86 to 0 mm/s along the rolling direction. The stick zone occurs from 2.63° to 1.27°. The roller adheres with the blank in stick zone, and the local sliding distance and sliding speed are close to zero in the stick zone. The forward slip zone is from 1.27° to 0°. In the forward slip zone, the points on the surface of the roller are sliding towards the neutral point. With a decreasing contact angle, the local sliding distance increases from 0 to 2.31 μm, and the local sliding speed increases from 0 to 2.29 mm/s opposite to the rolling direction. The sliding direction of the roller is the same as the rolling direction in the backward slip zone, however the sliding direction of the roller is opposite to the rolling direction in the forward slip zone, as shown in Figure 7b. The neutral angle is smaller than a half of the contact angle, as shown in Figure 7a. The forward slip zone is the smallest, taking up 30.5% of the contact surface of the rolling bite, followed by the stick zone (32.7%) and the largest is the backward slip zone which consumed 36.8% of the contact surface of the rolling bite according to Figure 7b.

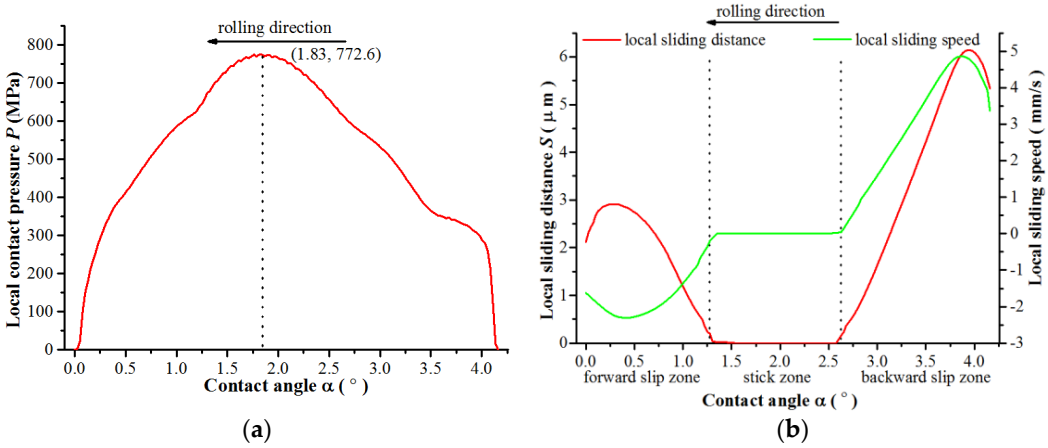

Figure 7. Distribution of local contact pressure (**a**) and local sliding (**b**) over the rolling bite.

It's difficult to accurately measure the local contact pressure and sliding distance by experiment. In order to validate the FEA model, firstly the simulated rolling force was compared with the experimental rolling force, as shown in Figure 8a. The rolling forces of the simulation and test reach peak values rapidly during the transient state. After that, the rolling force becomes a constant value during the steady-state rolling process. The simulated steady rolling force is only 6.9% bigger than the rolling force of the measured value. In addition, an analytic result of local contact pressure was compared with the simulated results, as shown in Figure 8b. The Karman equation is an analytic method for calculating the local contact pressure [19]. The theory divided the rolling bite into forward and backward slip zones, and the local contact pressure in forward and backward slip zone were calculated by Equation (2a,b), respectively.

$$P_h = \frac{K}{\delta}\left[(\delta+1)\left(\frac{h_x}{h}\right)^{\delta} - 1\right] \tag{2a}$$

$$P_H = \frac{K}{\delta}\left[(\delta-1)\left(\frac{H}{h_x}\right)^{\delta} + 1\right] \tag{2b}$$

where P_h and P_H are the local contact pressure in the forward and backward slip zone, K is the flow stress and $K = 1.15\,\sigma_s$, σ_s is the yield strength of blank, $\delta = \frac{2lf}{H-h}$, l is the length of rolling bite, f is the friction coefficient, H is the thickness of blank, h is the thickness of plate, h_x is the local thickness of the plate on rolling bite. Figure 8b shows that both analytic solution and simulated local contact pressure in rolling bite distribute as a hill-shaped profile. The locations of the peak contact pressure from both methods are barely 2% different and the amplitude of simulated local contact pressure is 11.8% bigger than the analytical result. Overall, the FEA agrees with the analytic solution. The diffidence might be due to the assumptions taken in the analytical solution to obtain Equation (2a,b),. The two validations indicate that the numerical model presented in Section 2.3 is a valid representation of the plate rolling process. Meanwhile, Weisz-Patrault et al. [19] used optical fiber Bragg gratings sensors to measure the contact stresses of a rolling bite, and Chen et al. [23] studied the local contact pressure of a rolling bite in a hot rolling process based on Karman equation. Both of the publication showed similar distribution of local contact pressure, as shown in Figures 6a and 8b.

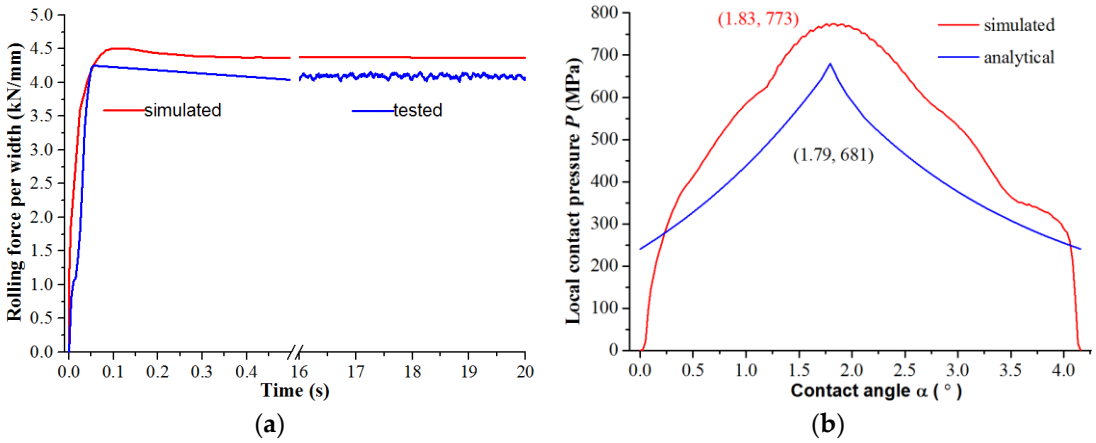

Figure 8. Validation of FEA model. (**a**) Comparison of rolling force per unit width between simulation and experimental test, (**b**) comparison of simulated local contact pressure with analytical results.

3.2. Rolling Parametric Study

Considering the wear performance of a roller during the rolling process, it is believed that local contact pressure and sliding over contact surface are of particular importance [24]. The local contact condition depends on the shapes, the materials and the relative motion of the contact pairs as highlighted in Section 2. Therefore, the investigation of rolling parameters can aid in understanding the contact and wear response of a rolling process. Moreover, this will facilitate a possible reduction in roller wear, via a reduction in peak contact pressure and sliding distance through optimizing parameters [6]. In a steady-state process for a symmetric rolling process, the local contact pressure P and local sliding distance S at the location α in the rolling bite are dependent on the parameters in Equation (3a,b), respectively.

$$P = F(\alpha, h, \varepsilon, d, f, \omega,\ M_B, M_R) \tag{3a}$$

$$S = F(\alpha, \Delta t, h, \varepsilon, d, f, \omega,\ M_B, M_R) \tag{3b}$$

where h is thickness reduction of the plate, ε is the thickness reduction, d is the diameter of roller, f is the friction coefficient, ω is the angular speed of the roller, Δt as defined in Section 2.3 is the time increment for calculating S. M_B is material property of the blank, M_R is material property of the roller. It is worth mentioning that Equation (3a,b) indicate that local contact pressure P and local sliding distance S depend on the roller's diameter. If the accumulated wear is so severe that the roller's diameter has reduced significantly, then the roller's diameter should be updated in the consequent analysis. The plate thickness depends on the requirement of the produced component,

which was chosen to be 1.5 mm in this paper. Only the steady-state portion of the plate rolling process is considered and therefore the effect of the angular velocity of the roller is neglected. The parameters shown in Table 3 were investigated in this paper, and a parametric study was carried out by varying a specified parameter while fixing the values of the other parameters to investigate the effect of these parameters on the local contact responses.

Table 3. Parameters for the investigation.

Parameters	Values Considered
Thickness reduction (%)	15, 20, 25, 30, 35
Radius of roller (mm)	90, 140, 190, 240, 290
Friction coefficient	0.15, 0.20, 0.25, 0.30, 0.35
Material of blank	AZ31, Al7050, TC4, GH4169
Material of roller	9Cr2Mo, Cr15, A532M, 12Cr2Ni4, QT900

3.2.1. Effect of Thickness Reduction (ε)

Different thickness reduction determines the stands group for rolling [9]. More stands groups are needed if a smaller thickness reduction is used. A bigger thickness reduction induces larger plastic deformation and may cause cracks on the plate due to the larger rolling contact pressure and sliding. The larger contact pressure and sliding also induce more severe wear on the roller. The local contact pressure and sliding distance were simulated using different thickness reduction while the values of other parameters were kept the same, and the results are shown in Figure 9. When the thickness reduction was increased from 15% to 35%, the length of rolling bite increased and the relative location of the neutral point moved far away from the exit section of the rolling process, which is consistent with findings by Chen et al. [23] and Gao et al. [25]. The local contact pressure has a hill-shaped profile and the magnitude of the peak increased significantly from 619 to 903 MPa, because of the larger plastic deformation of the blank, which led to a larger deforming resistance of the roller [26]. Meanwhile, the local sliding distance curve has double peaks. When the thickness reduction was increased from 15% to 35%, the maximum of the local sliding distance increased from 2.6 to 9.8 μm in backward slip zone, and the maximum local sliding distance increased from 1.7 to 4.3 μm in forward slip zone. The local sliding was more severe in backward slip zone than that in forward slip zone. When the thickness reduction was increased, the length of the rolling bite increased and the difference between the roller's and the blank's speed at the entry section also increased. The forward slip rate increased with the increase in thickness reduction, which was also observed by Li et al. [27].

The plate was deformed by extrusion forces from the rollers, and springback occurred after plastic deformation. The contact pressure in the forward slip zone can be regarded as the load from the roller to resist the plate's springback. The resistance from the roller was constant at the forward slip zone because the plate thickness was unchanged even if the thickness reduction increased (Figure 9). However, the resistance from the roller increased in the backward slip zone with the increase of the thickness reduction because the blank thickness was increased. This means that the neutral point moved towards exit section and the rate which represents relative location decreased with the increase of the thickness reduction, as shown in Figure 10a. Kazeminezhad and Taheri [17] studied rolling pressure distribution and investigated the variation of the location of the neutral point. Their results showed that the neutral angle increased with the increase of the thickness reduction. However, the increment of neutral angle was smaller than the increment of total rolling bite, which was confirmed by the result in Figure 10a. When the thickness reduction increased, the percentage of the forward slip zone increased slightly and the backward slip zone was increased significantly because the loading and length of rolling bite increased. The percentage of stick zone decreased significantly because the percentages of both the forward and backward slip zone increased, shown in Figure 10b. This agrees with the analytical model proposed by Minton et al. [28].

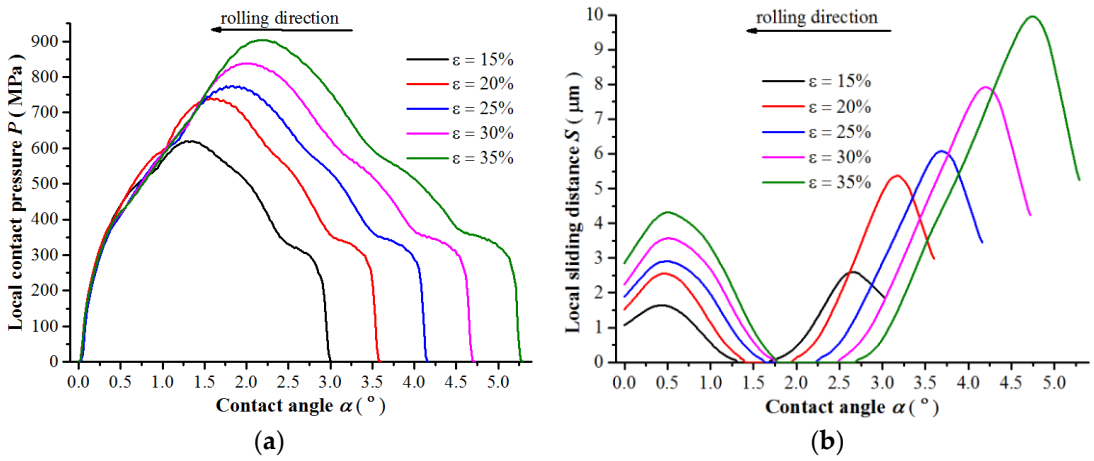

Figure 9. Contact pressure (**a**) and local sliding distance (**b**) distribution over the rolling bite with different thickness reduction (other parameters were constant with h = 1.5 mm, d = 190 mm, f = 0.25, AZ31, A532M).

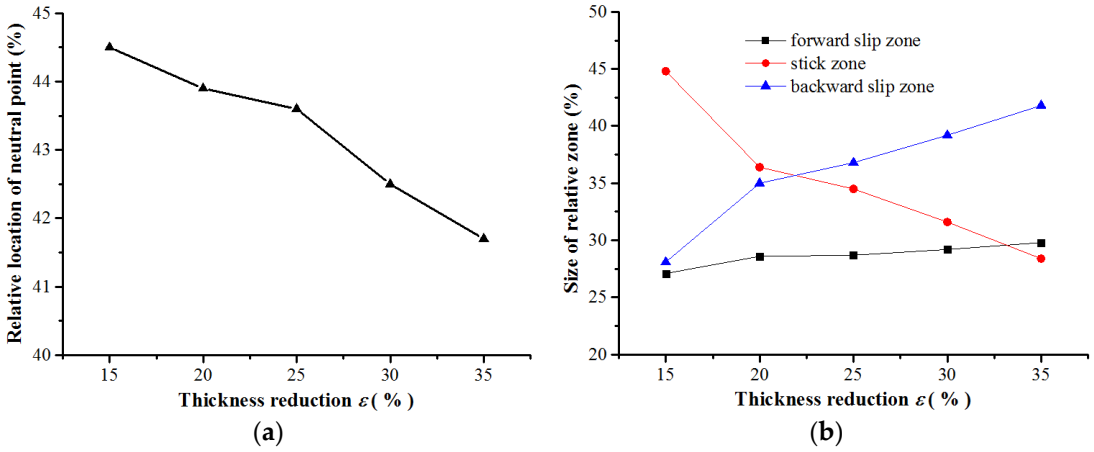

Figure 10. Relative location of the neutral point (**a**), and percentage of the stick and slip zones (**b**) in rolling bite with the different thickness reduction (other parameters were constant with h = 1.5 mm, d = 190 mm, f = 0.25, AZ31, A532M).

3.2.2. Effect of Roller's Diameter (d)

The diameter of the roller is also an important parameter for the rolling process. The local contact pressure and sliding distance were simulated using different roller diameters, while the values of the other parameters were unchanged. The simulation results are shown in Figure 11. When the roller diameter was increased from 90 to 290 mm, the length of the rolling bite was increased from 4.8 to 8.5 mm and the angle of rolling bite decreased from 6.04° to 3.37°. While angular speed was constant, the forming speed at the exit section increased when the diameter of the roller increased. The local contact pressure had a hill-shaped profile and the magnitude of the peak increased significantly from 555 to 984 MPa. The increase in the contact pressure is due to the increase in the rolling force. For the same thickness reduction, a larger roller leads to a longer roller bite and needs a larger rolling force. The local sliding distance curve had double peaks, as shown in Figure 11b. The maximum of the local sliding distance increased from 5.37 to 6.23 μm in the backward slip zone, and the maximum of the local sliding distance increased from 2.3 to 3.5 μm in the forward slip zone. Figure 11b shows that more severe sliding occurred when using a bigger diameter roller, because the length of rolling bite and rolling force increased.

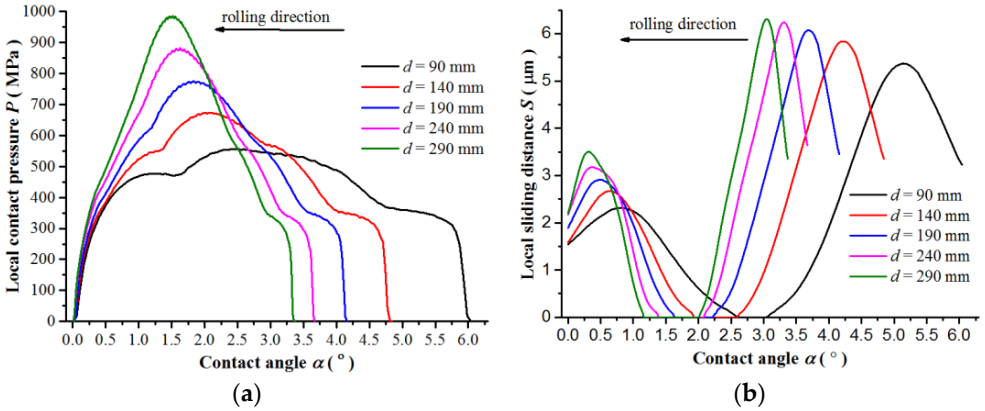

(**a**) (**b**)

Figure 11. Contact pressure (**a**) and local sliding distance (**b**) distribution over the rolling bite with different diameters of the roller (other parameters were constant with h = 1.5 mm, ε = 25%, f = 0.25, AZ31, A532M).

According to the numerical results, the relative location of the neutral point in rolling bite was about 43.8%, which was unchanged with the variation of diameter of the roller, as shown in Figure 12a. This is consistent with the study by Kijima [29,30]. When the diameter of the roller increased, the percentage of the forward slip zone was unchanged. The percentage of the stick zone increased slightly, and the percentage of backward slip zone decreased slightly, as shown in Figure 12b. The variation of roller's diameter changed the amplitude of the contact pressure and sliding distance, because the angle and length of the rolling bite changed.

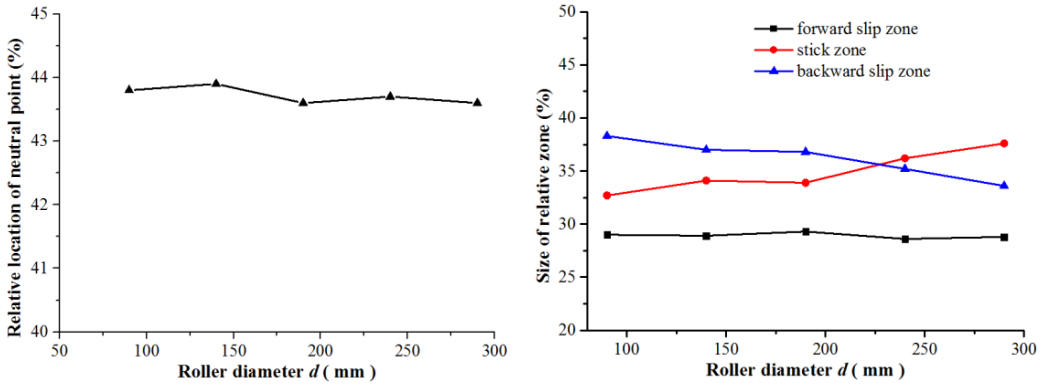

(**a**) (**b**)

Figure 12. Relative location of the neutral point (**a**), and percentage of the stick and slip zones (**b**) in rolling bite using the different diameter of roller (other parameters were constant with h = 1.5 mm, ε = 25%, f = 0.25, AZ31, A532M).

3.2.3. Effect of Friction Coefficient (f)

In a rolling process, the blank is driven into the gap between the rotating rollers by friction. Hence, friction coefficient is significant to the contact response. Figure 13 shows the predicted local contact pressure and local sliding distance of the roller with varying friction coefficients while the values of other parameters were kept constant. When the friction coefficient was increased from 0.15 to 0.35, the local contact pressure increased, and the magnitude of the contact pressure increased from 565 to 909 MPa, as shown in Figure 13a. Because the greater friction exacerbates the contact between roller and blank, the local contact pressure and rolling force increased (the rolling force perpendicular to rolling direction increased from 3.5 to 5.0 kN/mm). Hence, the hill-shaped profile of the local contact pressure was sharper, which was confirmed by Shahani et al. [31] and Yadav et al. [32]. The local sliding distance decreased in the backward slip zone, and the magnitude decreased from 7.28 to 5.15 μm. The intensified

contact impeded the sliding between the roller and the blank, hence, the sliding decreased in backward slip zone. However, the local sliding distance increased in forward slip zone, and the magnitude increased from 2.2 to 2.9 μm, as shown in Figure 13b. A bigger friction coefficient raised the values of forward slip and the plate's speed at exit section, which agrees with Wang et al. [33].

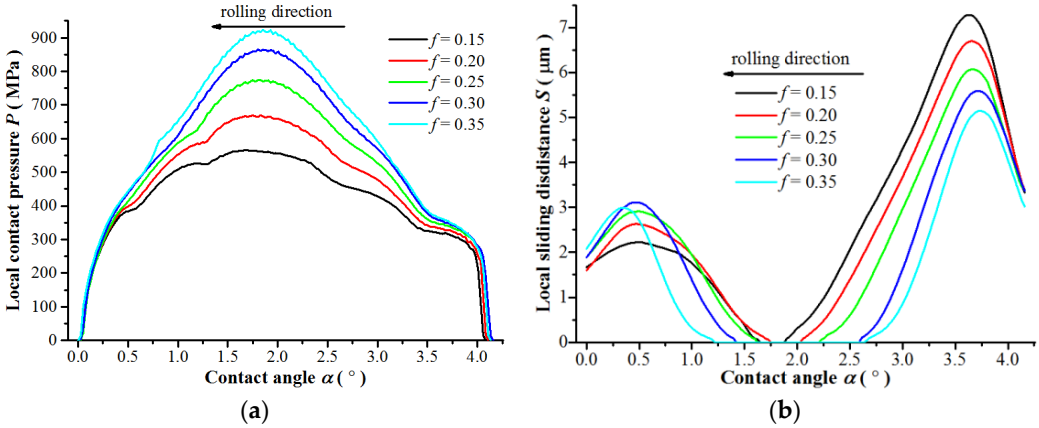

Figure 13. Contact pressure (**a**) and local sliding distance (**b**) distribution over the rolling bite with different friction coefficient (other parameters were constant with h = 1.5 mm, ε = 25%, d = 190 mm, AZ31, A532M).

According to the numerical result, the relative location of the neutral point in rolling bite was about 43.8%, as shown in Figure 14a. When the friction coefficient increased, the percentage of the stick zone was increased significantly, and the percentage of the forward slip zone and backward slip zone shrank, as shown in Figure 14b. The reason is that a higher friction coefficient enlarges the region of saturated friction, and many more nodes at the boundary of slipping zone stick with roller. Gao et al. obtained similar results [25].

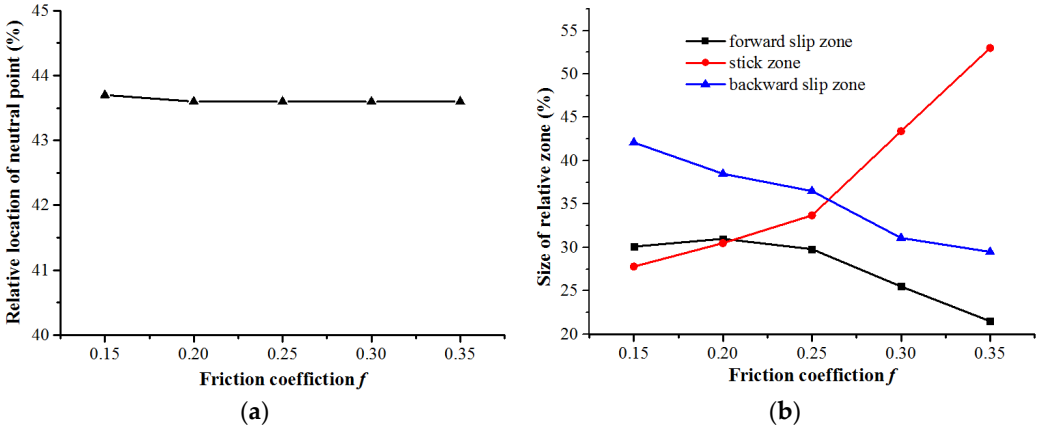

Figure 14. Relative location of the neutral point (**a**), and percentage of the stick and slip zones (**b**) in rolling bite with the different friction coefficient (other parameters were constant with h = 1.5 mm, ε = 25%, d = 190 mm, AZ31, A532M).

3.2.4. Effect of Blank's Material Property (M_B)

The local contact responses also depend on the material properties of the contact pieces. Four typical metals used in the aviation industry were investigated in this paper while the values of the other parameters were kept constant. The properties of these materials are shown in Table 4. As shown in Figure 15a,b, different blank materials have different local contact pressure and local sliding distance distributions. Referring to Table 4, Figure 15a indicates that a material with a higher strength, including

yielding strength and tensile strength, and a higher Yong's modulus tends to have a higher peak contact pressure, which is consistent with a previous study on contact pressure in sheet stamping [6].

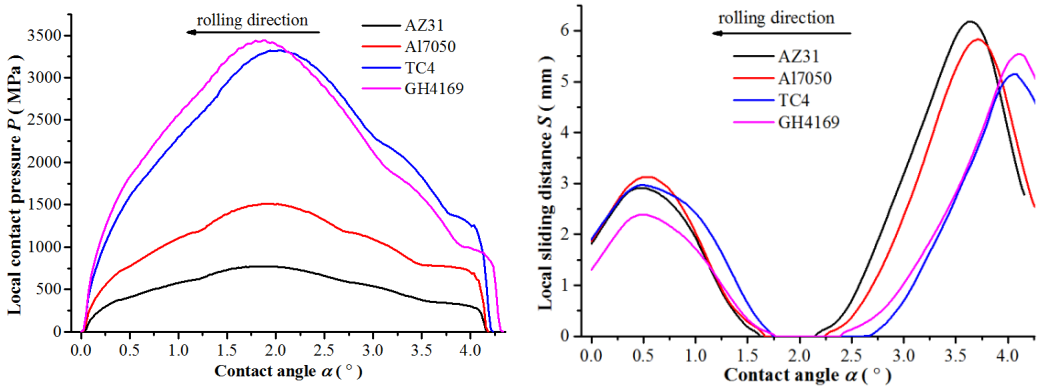

Figure 15. Contact pressure (**a**) and local sliding distance (**b**) distribution over the rolling bite with different material property of blank (other parameters were constant with h = 1.5 mm, ε = 25%, d = 190 mm, f = 0.25, A532M).

Table 4. Properties of four typical metals in aviation industry used in the parametric study.

Material properties	AZ31	Al7050	TC4	GH4169
Density (kg/m^3)	1780	2830	5100	8190
Young's modulus (GPa)	37.4	70.3	112	199.9
Poisson's Ratio	0.3	0.33	0.34	0.3
Yield strength (MPa)	140	455	887	550
Tensile strength (MPa)	311	510	950	965

Figure 16a shows that the relative location of the neutral point in rolling bite is about 43.8%. Hence, the contact pressure distribution was unchanged and the location of neutral point was unchanged. The percentage of the forward slip zone was unchanged for blanks of different materials. The percentage of the stick zone increased and the percentage of the backward slip zone decreased when using a material with a higher Young's modulus and tensile strength, as shown in Figure 16b. When the Young's modulus of blank increased, the blank was easier to achieve plastic deformation at the interface, hence, the backward slip zone shrunk and the stick zone enlarged.

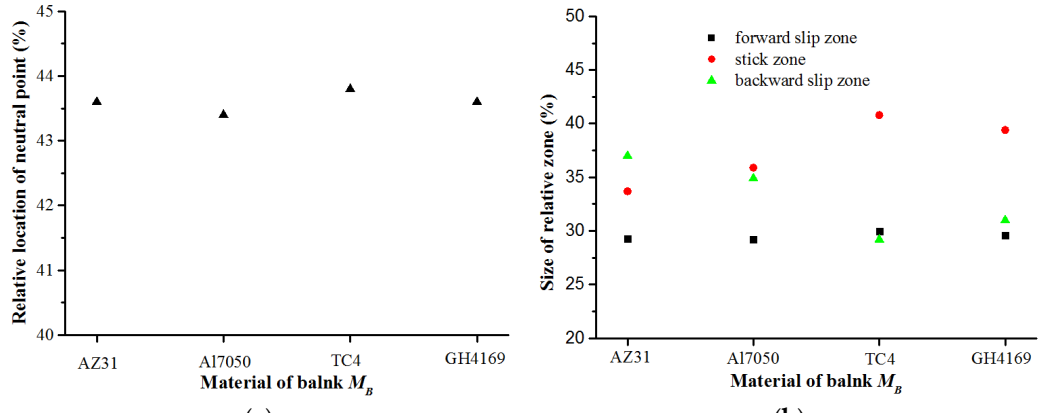

Figure 16. Relative location of the neutral point (**a**), and percentage of the stick and slip zones (**b**) in rolling bite with different material properties of blank (other parameters were constant with h = 1.5 mm, ε = 25%, d = 190 mm, f = 0.25, A532M).

3.2.5. Effect of Roller's Material Property (M_R)

The local contact response was also investigated for different rollers while the other parameters were kept constant. The typical materials used for rollers and their properties are listed in Table 5. Figure 17a shows the distributions of the local contact pressure for five roller materials. The difference between the contact pressure distributions among the five roller materials is not significant, due to the fact that their properties, as listed in Table 5, have no significant difference. The results indicate that the Young's modulus might play a dominate role among all the material property parameters, as the local contact pressure is higher for the roller material with a higher Young's modulus. A similar conclusion was obtained by Pereira et al. [6] in studying metal stamping. Figure 17b shows that the local sliding distance decreased in the backward slip zone and forward slip zone when the Young's modulus of roller increased. Figure 18a shows that the relative location of the neutral point in rolling bite decreased when the Young's modulus of roller decreased. The reason might be that the increase of local contact pressure induced shrink of forward slip zone, as shown in Figure 18b.

Figure 18a shows that the relative location of the neutral point in the rolling bite decreased slightly when the Young's modulus of the roller decreased. Because the deformation resistance of blank is a constant, the contact responses are more severe for a soft roller [34]. The percentage of the forward slip zone decreased slightly, and the percentage of the stick zone and backward slip zone are increased slightly, see Figure 18b. It is an evidence for the reduction of the rate which represent the relative location of the neutral point.

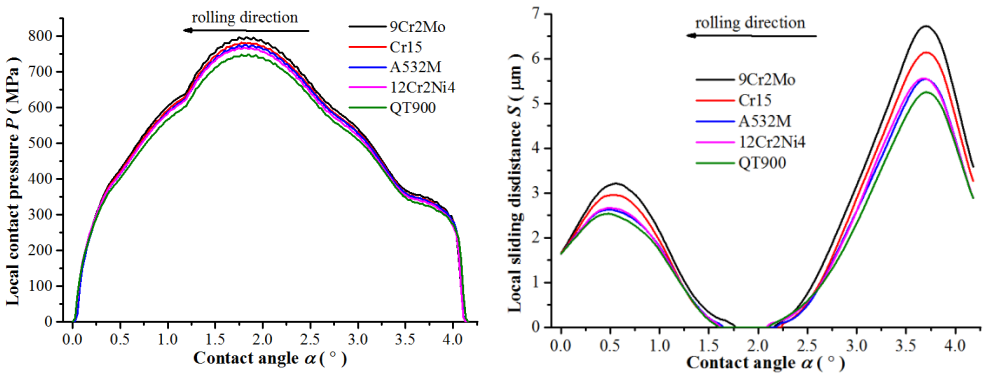

Figure 17. Contact pressure (**a**) and local sliding distance (**b**) distribution over the rolling bite with different material properties of roller (other parameters were constant with h = 1.5 mm, ε = 25%, d = 190 mm, f = 0.25, AZ31).

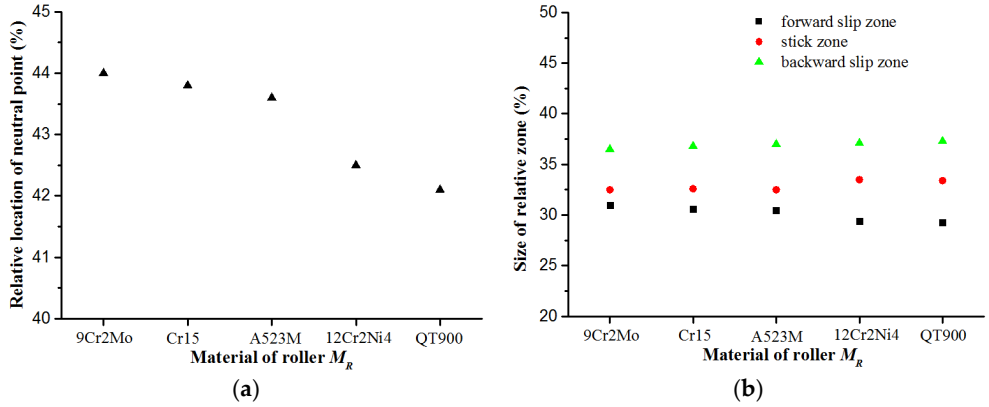

Figure 18. Relative location of the neutral point (**a**), and percentage of the stick and slip zones (**b**) in rolling bite with different material property of roller (other parameters were constant with h = 1.5 mm, ε = 25%, d = 190 mm, f = 0.25, AZ31).

Table 5. Properties of 5 roller materials for cold rolling used in the parametric study.

Material Properties	9Cr2Mo	Cr15	A532M	12Cr2Ni4	QT900
Density (kg/m^3)	7810	8470	7850	7840	7180
Young's modulus(GPa)	236	219	215.6	207	181
Poisson's Ratio	0.3	0.3	0.3	0.29	0.27

The local contact pressure and local sliding distance are complex responses in a rolling process, however, the contact condition responses are similar in the three zones. The contact pressure over the rolling bite presents a "hill shape" profile, and the peak value occurred at neutral point. The local sliding distance over the rolling bite presents a "double peak" profile. The slight local sliding occurred in forward slip zone. Severe local sliding occurred in backward slip zone. The parametric study showed that the local contact pressure and sliding distance increased when the thickness reduction or diameter of roller increased. The location of neutral point was near the center of the rolling bite. The size of forward slip zone is usually stable and smaller than one third of the rolling bite, only if the thickness reduction or the material of roller is changed. The size of the stick zone is nearly one third of the rolling bite, and it can only enlarge significantly if the friction coefficient increases. The size of the backward slip zone usually is bigger than one third of the rolling bite. The size of the stick zone enlarges and the slip zones shrink significantly when the friction coefficient increases. The parametric study showed that the material of the blank had the most important impact on the local contact pressure. The thickness reduction had the most important impact on the local sliding and the relative location of the neutral point. The friction coefficient had the most important impact on the size of the stick and slip zones. According to the parametric study, if the thickness reduction and materials of roller and blank are fixed, when the diameter of roller increase, the local contact pressure and sliding distance increases, the size of stick zone increases and the size of backward slip zone slightly decreases. When the friction coefficient increases, the local contact pressure increases, the local sliding distance increases in the backward slip zone and decreases in the forward slip zone, the size of stick zone enlarges and the size of slip zone shrinks. The complex contact response on the roller induces local wear, and the local wear of roller can be examined based on Equation (1), which is presented in the following section.

4. Wear Prediction of the Roller

An insight into the possible wear behavior over the rolling bite can be obtained based on the numerical results. In the steady-state rolling process, the distribution of the contact response and sliding over rolling bite are independent of time. Hence, the accumulated local wear in the rolling bite represents the total wear of any point in the roller in one cycle. The main purpose of this paper is to show the possible trend of wear in the rolling bite by utilizing the knowledge of the contact conditions which can be obtained through FEA. For this reason, the wear coefficient k in Equation (1) was treated as a constant and its effect was excluded in the discussion for a given pair of materials. The following discussion only considers the case of given blank material as AZ31 and the roller material as A532M, which are presented in Section 2.1. The wear response of the roller can be quantitatively determined by combining local contact pressure and local sliding distance, which is defined in Figure 6. According to Equation (1), the local nominal wear intensity w_n can be described as

$$w_n = \frac{W}{k} = P^m S^n \tag{3}$$

The total nominal wear (per unit width as it is a plane strain problem) on the roller during the rolling time period Δt corresponding to the sliding distance, which was introduced in Section 2.3, can be calculated by

$$W_{\Delta t} = \int_0^{\alpha_C} \frac{d}{2} w_n d\alpha = \frac{d}{2} \int_0^{\alpha_C} w_n d\alpha \tag{4}$$

where α_C is the angular size of the contact region, that is, the rolling bite. It is worth noting that the integration of Equation (5) is carried out over the rolling bite to obtain the wear for the whole roller because wear only occurs in the rolling bite. Therefore, the total nominal wear of the whole roller (per unit width) during one rolling cycle is

$$W = \frac{2\pi}{\omega \Delta t} w_{\Delta t} = \frac{\pi d}{\omega \Delta t} \int_0^{\alpha_C} w_n d\alpha \tag{5}$$

It is worth commenting that the reduction of the roller due to accumulated wear doesn't affect the application of Equation (4) to analyze the wear intensity or the application of Equation (6) to analyze the wear per one rolling cycle. However, the roller size should be updated in the estimation of the accumulated wear due to rolling cycles. An insight into the wear behavior of the roller for one rolling cycle can be obtained based on Equations (4)–(6). Although the empirical constants in Equation (4) are usually fitted using data obtained from simulated laboratory test, in general, it has been observed that $m \geq 1$ (with typical values in the range of 1–3), and $n \leq 1$ [6]. Hence, the values of m and n are chosen within these ranges in the following discussion. According to the local contact pressure and local sliding distance presented in Figure 7, the distribution of the local nominal wear response can be obtained by using Equation (4), and the total nominal wear of the roller over one rolling cycle can be obtained by using Equation (6). The results are presented in Figure 19 with different empirical constants.

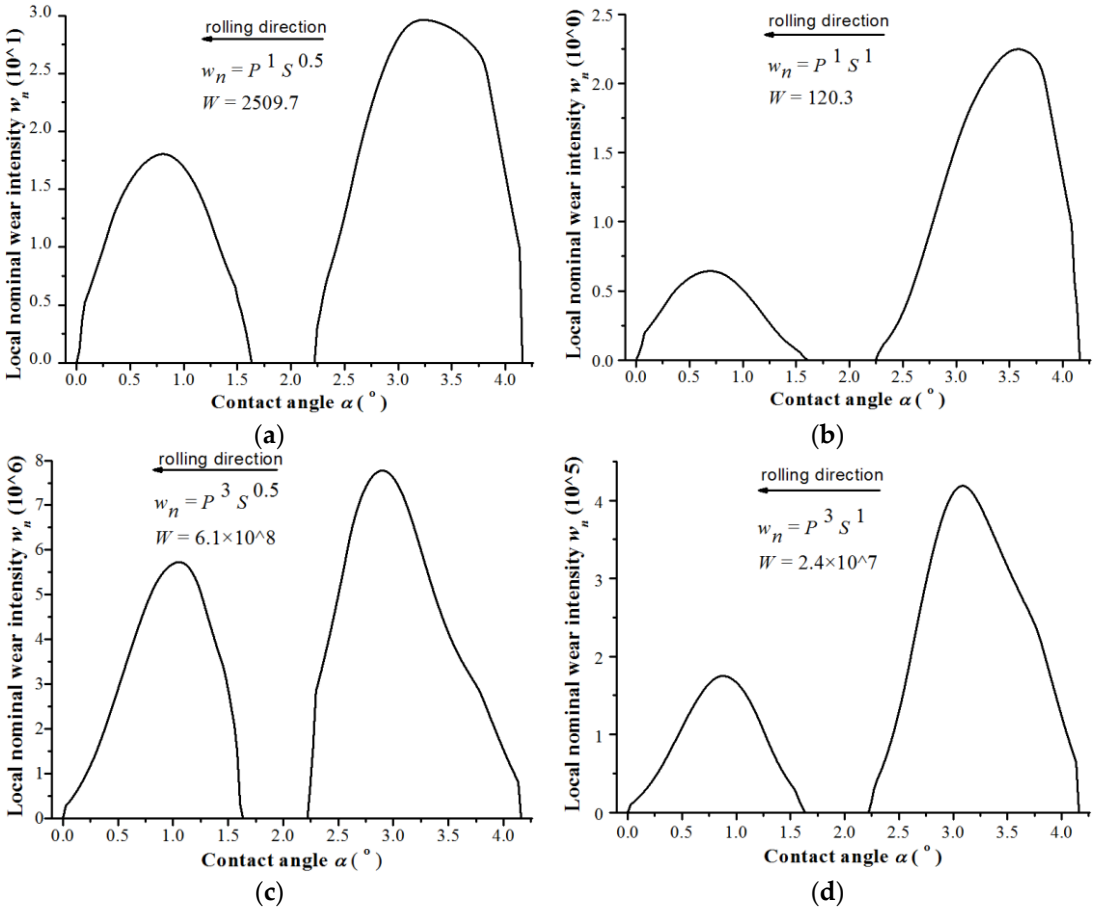

Figure 19. Local nominal wear intensity distribution over the rolling bite with different wear exponent values: (**a**) $m = 1$, $n = 0.5$; (**b**) $m = 1$, $n = 1$; (**c**) $m = 3$, $n = 0.5$; (**d**) $m = 3$, $n = 1$.

Figure 19 shows a typical two-peak wear response that exists in the backward and forward slip zone. The magnitude of the wear peak of the backward slip zone is bigger than that of the forward slip zone in all the four cases. Considering the results presented in Figure 7b, it is evident that the roller surface over the rolling bite experiences significant sliding in the backward slip zone and less sliding in the forward slip zone. Hence, there is severe wear present in the backward slip zone and less wear present in the forward slip zone.

In order to improve the performance life of the roller, the local wear can be reduced by decreasing the local sliding distance, local contact pressure, or the percentage of the slip zones. The impacts of parameters on the local nominal wear intensity were investigated based on Equation (4). The empirical constants m and n are held constant (m = 1, n = 1). For cold rolling AZ31 (material of blank) by A532M (material of roller), the thickness reduction, diameter of roller and the friction are presented in Table 3, the local contact pressure and sliding distance are shown in Figures 9–13 respectively. The local nominal wear are shown in Figure 20. Meanwhile, the total nominal wear per unit area on roller during one rolling process is also investigated based on Equation (6). The results are shown in Figure 21.

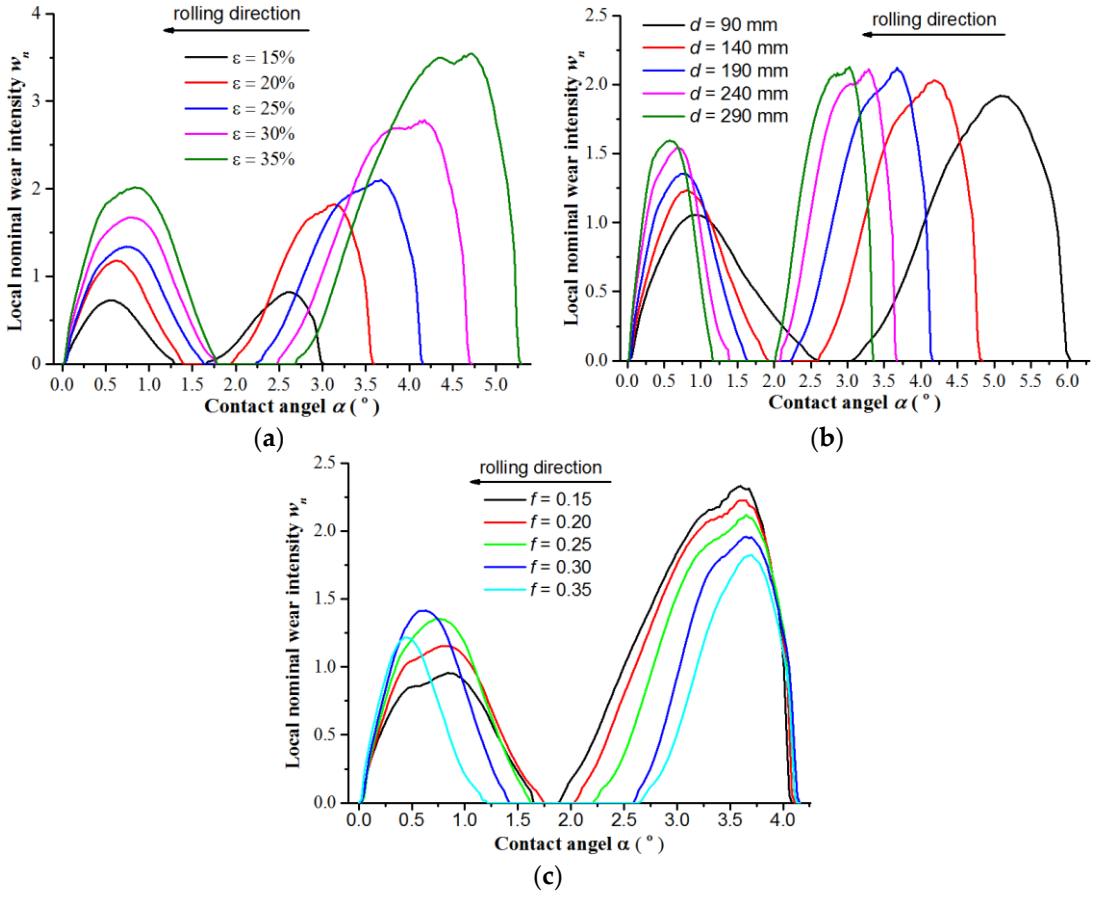

Figure 20. Local nominal wear intensity over the rolling bite with the different rolling parameters (m = 1, n = 1). (**a**) Local nominal wear with the different thickness reductions; (**b**) Local nominal wear with the different rollers' diameters; (**c**) Local nominal wear with the different friction coefficients.

For different empirical constants m and n in the Equation (4), the magnitudes of the local nominal wear vary significantly, as shown in Figure 19. Hence, the magnitude of the total nominal wear per rolling cycle changes greatly. In order to investigate the wear of roller when using different empirical constants m and n, the total nominal wear of the roller per rolling cycle is normalized by its value when using the same constant m and n with the standardized parameters (ε = 25%, d = 190 mm, f = 0.25). The normalized wear results are shown in Figure 22. Meanwhile, the total nominal wear of the roller

was considered using the different thickness reduction and diameter of roller for producing same rolled plates, the results are shown in the insets of Figure 22a,b.

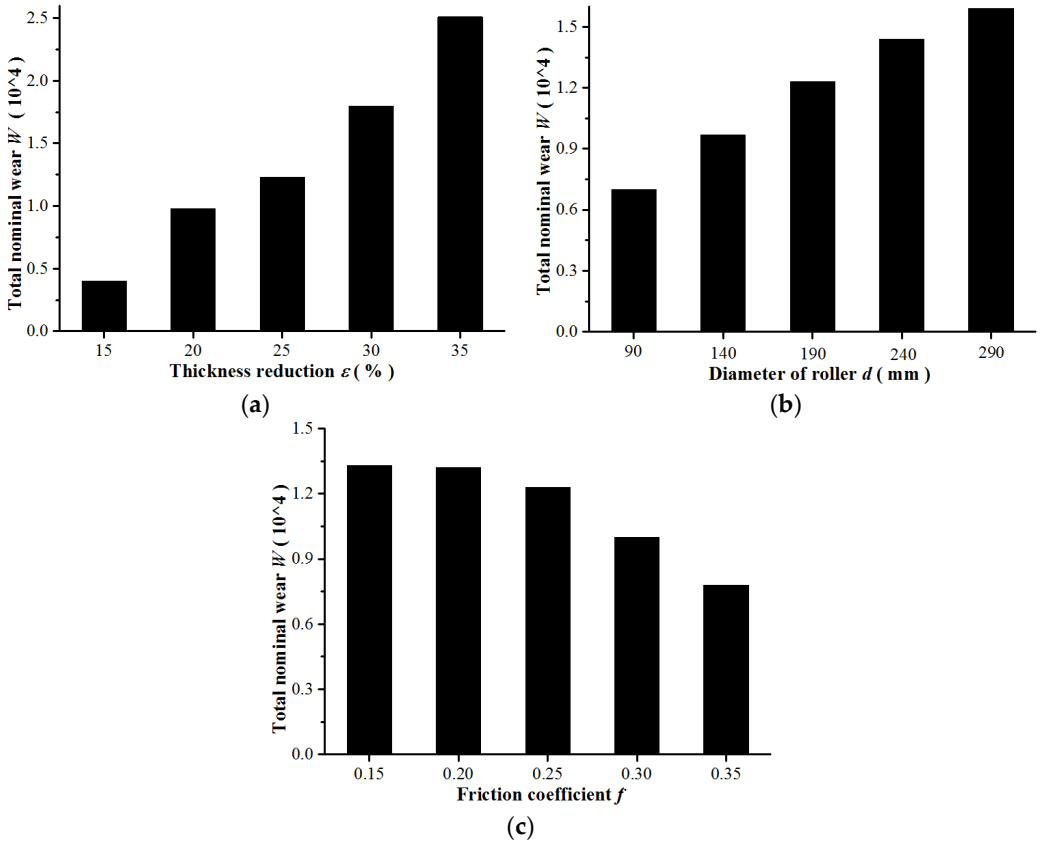

Figure 21. Total nominal wear per unit on the roller during one rolling process. (**a**) Total nominal wear with the different thickness reductions; (**b**) Total nominal wear with the different rollers' diameters; (**c**) Total nominal wear with the different friction coefficients.

The thickness reduction is the most important parameter in the nominal wear intensity and the nominal wear per rolling cycle, which are demonstrated in Figures 20a, 21a and 22a, respectively. The total nominal wear per rolling cycle is smaller when using a smaller thickness reduction, because a larger thickness reduction induces higher local contact pressures and large local sliding, which is shown in Figure 9. In the rolling industry, more rolling stands groups are needed when using a smaller thickness reduction. For example, when using thickness reduction ε = 15%, 20%, 25%, 30% and 35% respectively to a rolling process with 90% total thickness reduction, the rolling stands groups are 14, 10, 8, 6 and 5. Wear on the roller surface accumulates with increasing the rolling stands groups. Considering the number of rolling stand groups to produce a plate with the same reduced thickness, according to the inset of Figure 22a, the accumulated nominal wear to complete the rolling task is smaller when using a smaller thickness reduction.

The roller diameter is the second important parameter to the nominal wear intensity and the nominal wear per rolling cycle, as demonstrated in Figures 20b, 21b and 22b receptively. The nominal wear per rolling cycle is smaller when using a smaller diameter roller. The roller diameter also changes the shape and length of the rolling bite, and the local contact pressure and sliding distance change significantly, as shown in Figure 11. A larger diameter roller produces a longer plate in one rolling cycle, and the total nominal wear per unit width of the roller during one rolling cycle can be calculated by Equation (6). Comparing the accumulated nominal wear for rolling the same length plate, the inset of Figure 22b shows that less wear occurs when using a smaller diameter roller, although, the difference is not significant.

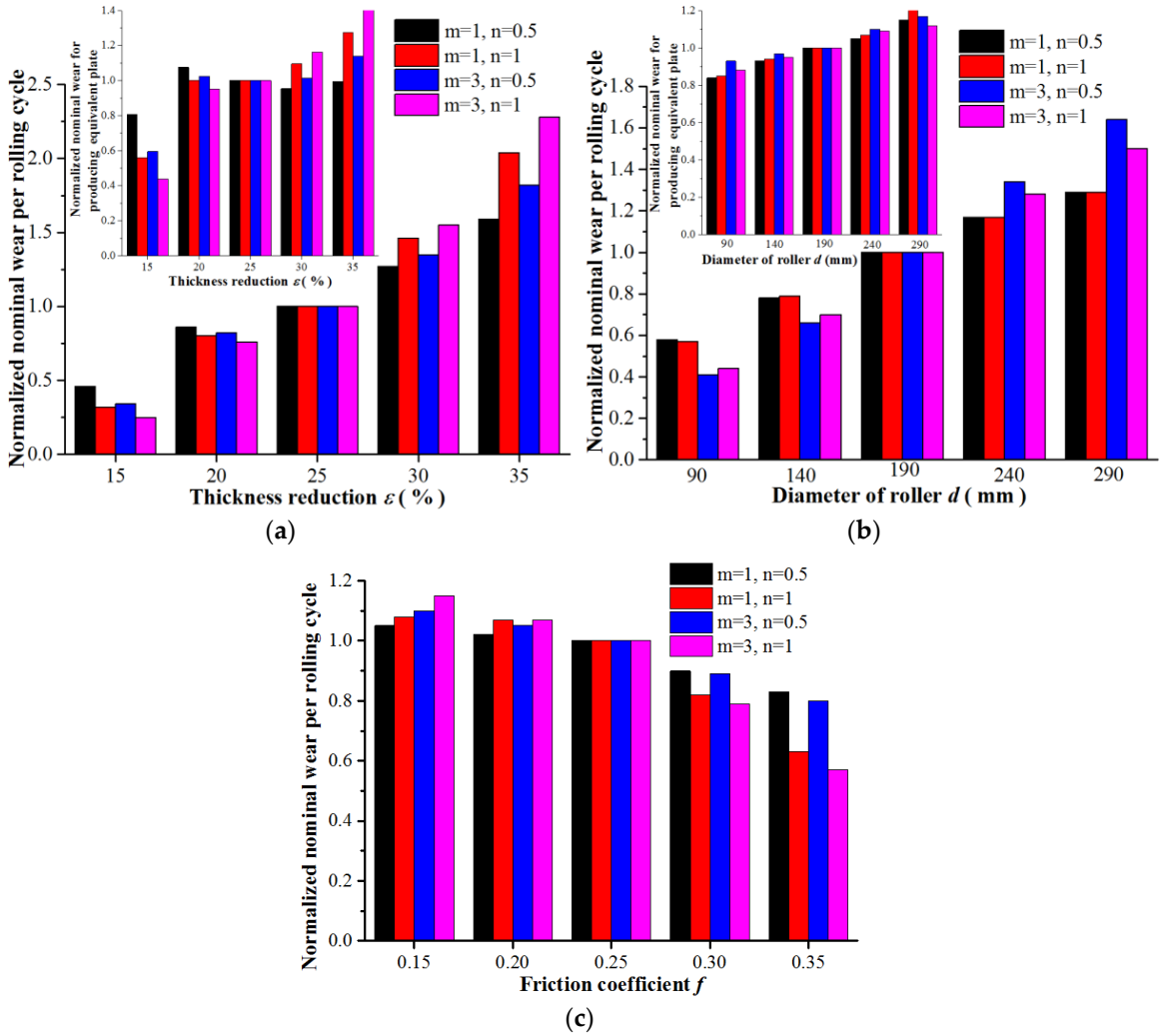

Figure 22. Normalized nominal wear of the roller during one rolling process. (**a**) Normalized nominal wear for one rolling cycle and producing equivalent plate using the different thickness reductions, (**b**) Normalized nominal wear for one rolling cycle and producing equivalent plate using the different rollers' diameters, (**c**) Normalized nominal wear using the different friction coefficients.

The friction coefficient is the third important parameter to the nominal wear intensity and the total nominal wear per rolling cycle, as demonstrated in Figures 20c, 21c and 22c. The total nominal wear per rolling cycle is smaller if the friction coefficient is higher. This finding can be explained by the fact that the stick zone increases and the two slip zones shrink if the friction coefficient increase, as shown in Figure 14b. As a result, the local wear intensity decreases in the forward slip zone, as shown in Figure 20c.

According to the parametric study, when the materials of blank and roller are given, it is possible to prolong the life of the roller by using a lower thickness reduction, a smaller diameter roller and having a contact surface with a larger friction coefficient.

5. Conclusions

This paper developed an understanding of the rolling contact condition and the wear response of the roller in cold rolling based on FEA. It was the first study to quantify the local sliding distance in a rolling by using FEA. The concept of wear intensity was introduced and applied to examine rolling wear. The major findings are summarized below.

1. The local contact pressure over the rolling bite demonstrates a hill-shape profile, and the peak of local contact pressure occurs at the neutral plane. The rolling bite is divided into the forward slip zone, the stick zone and the backward slip zone. The local sliding distance demonstrates a double-peak profile. The magnitude of local sliding distance in the backward slip zone is larger than that in the forward slip zone.

2. The results of the parametric study show that the local contact pressure and sliding distance increase when the thickness reduces or roller diameter increases. When the friction coefficient increases, the local contact pressure increases over the rolling bite, the local sliding distance increases in the backward slip zone and decreases in the forward slip zone. The location of the neutral plane is always at the rolling exit side of the rolling bite's center. The stick zone increases and the forward/backward slip zones shrink significantly when the friction coefficient increases.

3. Local wear intensity of the roller was estimated based on the local contact pressure and the local sliding distance. A typical two-peak wear response exists in the backward and forward slip zones.

4. For a given roller and blank material combination, using a smaller thickness reduction, a smaller diameter roller and having a rolling contact surface with a larger friction coefficient can reduce the wear of the roller.

Acknowledgments: This work was supported by the National Natural Science Foundation of China (No. 51475374), the Fundamental Research Funds for the Central Universities (No. 3102015ZY087). Qichao Jin acknowledges the financial support from the China Scholarship Council for a one-year visit at Monash University.

Author Contributions: Qichao Jin and Wenyi Yan designed, conducted the research and wrote the paper; Wenhu Wang and Ruisong Jiang discussed the research and editing the paper; Louis Ngai Sum Chiu assisted the FEA simulations; Di Liu tested the material property of AZ31.

Conflicts of Interest: The authors declare no conflict of interest.

References

1. Yan, Y.X.; Sun, Q.; Chen, J.J.; Pan, H.L. Effect of processing parameters on edge cracking in cold rolling. *Mater. Manuf. Process.* **2015**, *30*, 1174–1178. [CrossRef]
2. Chang, S.; Pyun, Y.S.; Amanov, A. Wear enhancement of wheel-rail interaction by ultrasonic nanocrystalline surface modification technique. *Metals* **2017**, *10*, 188. [CrossRef] [PubMed]
3. Abdo, J. Materials sliding wear model based on energy dissipation. *Mech. Adv. Mater. Struct.* **2015**, *22*, 298–304. [CrossRef]
4. Lavella, M. Contact properties and wear behaviour of nickel based superalloy rené 80. *Metals* **2016**, *6*, 159. [CrossRef]
5. Meng, H.C.; Ludema, K.C. Wear models and predictive equations: Their form and content. *Wear* **1995**, *181*, 443–457. [CrossRef]
6. Pereira, M.P.; Yan, W.Y.; Rolfe, B.F. Contact pressure evolution and its relation to wear in sheet metal forming. *Wear* **2008**, *265*, 1687–1699. [CrossRef]
7. Pereira, M.P.; Yan, W.Y.; Rolfe, B.F. Sliding distance, contact pressure and wear in sheet metal stamping. *Wear* **2010**, *268*, 1275–1284. [CrossRef]
8. Pereira, M.P.; Yan, W.Y.; Rolfe, B.F. Wear at the die radius in sheet metal stamping. *Wear* **2012**, *274–275*, 355–367. [CrossRef]
9. Szota, P.; Mroz, S.; Stefanik, A.; Dyji, H. Numerical modelling of the working rolls wear during rods rolling process. *Arch. Metall. Mater.* **2011**, *56*, 495–501. [CrossRef]
10. Mattei, L.; Puccio, F.D. Influence of the wear partition factor on wear evolution modelling of sliding surfaces. *Int. J. Mech. Sci.* **2015**, *99*, 72–88. [CrossRef]
11. Archard, J.F. Contact and Rubbing of Flat Surfaces. *J. Appl. Phys.* **1953**, *24*, 981–988. [CrossRef]
12. Hsu, S.M.; Shen, M.C.; Ruff, A.W. Wear prediction for metals. *Trinol. Int.* **1997**, *30*, 377–383. [CrossRef]
13. Hsiang, S.H.; Lin, S.L. Application of 3D FEM-slab method to shape rolling. *Int. J. Mech. Sci.* **2001**, *43*, 1155–1177. [CrossRef]
14. Salimi, M.; Sassani, F. Modified slab analysis of asymmetrical plate rolling. *Int. J. Mech. Sci.* **2002**, *44*, 1999–2023. [CrossRef]

15. Zhang, S.H.; Zhao, D.W.; Gao, C.R.; Wang, G.D. Analysis of asymmetrical sheet rolling by slab method. *Int. J. Mech. Sci.* **2012**, *65*, 168–176. [CrossRef]
16. Dong, Y.G.; Song, J.F. Research on the characteristics of forward slip and backward slip in alloyed bar rolling by the round-oval-round pass sequence. *Int. J. Adv. Manuf. Tech.* **2016**, *87*, 3605–3617. [CrossRef]
17. Kazeminezhad, M.; Taheri, A.K. Calculation of the rolling pressure distribution and force in wire flat rolling process. *J. Mater. Process. Technol.* **2006**, *171*, 253–258. [CrossRef]
18. Dong, Q.; Zhou, K.; Chen, W.W.; Fan, Q. Partial slip contact modeling of heterogeneous elasto-plastic materials. *Int. J. Mech. Sci.* **2016**, *114*, 98–110. [CrossRef]
19. Weisz-Patrault, D.; Maurin, L.; Legrand, N.; Salem, A.B.; Bengrir, A.A. Experimental evaluation of contact stress during cold rolling process with optical fiber bragg gratings sensors measurements and fast inverse method. *J. Mater. Process. Technol.* **2015**, *223*, 105–123. [CrossRef]
20. Dong, Y.G.; Song, J.F.; Luo, G.L.; Ren, Z.C. Mathematical model of neutral line on the contact zone in alloyed bar rolling by the round-oval-round pass sequence. *Int. J. Mech. Sci.* **2016**, *115–116*, 180–189. [CrossRef]
21. Jiang, Z.Y.; Tieu, A.K.; Lu, C.; Sun, W.H. A three-dimensional thermo-mechanical finite element model of complex strip rolling considering sticking and slipping friction. *J. Mater. Process. Technol.* **2001**, *125*, 649–656. [CrossRef]
22. Chumak, K.; Malanchuk, N.; Martynyak, R. Partial slip contact problem for solids with regular surface texture assuming thermal insulation or thermal permeability of interface gaps. *Int. J. Mech. Sci.* **2014**, *84*, 138–146. [CrossRef]
23. Chen, S.; Li, W.; Liu, X. Calculation of rolling pressure distribution and force based on improved Karman equation for hot strip mill. *Int. J. Mech. Sci.* **2014**, *89*, 256–263. [CrossRef]
24. Datta, A.K.; Das, G.; De, P.K.; Ramachandrarao, P.; Mukhopadhyaya, M. Finite element modeling of rolling process and optimization of process parameter. *Mat. Sci. Eng. A-Struct.* **2006**, *426*, 11–20. [CrossRef]
25. Gao, H.; Ramalingam, S.C.; Barber, G.C.; Chen, G. Analysis of asymmetrical cold rolling with varying coefficients of friction. *J. Mater. Process. Technol.* **2002**, *124*, 178–182. [CrossRef]
26. Ma, C.Q.; Hou, L.G.; Zhang, J.S.; Zhuang, L.Z. Influence of thickness reduction per pass on strain, microstructures and mechanical properties of 7050 Al alloy sheet processed by asymmetric rolling. *Mater. Sci. Eng. A-Struct.* **2015**, *650*, 454–468. [CrossRef]
27. Li, E.B.; Tieu, A.K.; Yuen, W.Y.D. Forward slip measurements in cold rolling by laser doppler velocimetry: Uncertainty analysis and accuracy improvement. *J. Mater. Process. Technol.* **2003**, *133*, 348–352. [CrossRef]
28. Minton, J.J.; Cawthorn, C.J.; Brambley, E.J. Asymptotic analysis of asymmetric thin sheet rolling. *Int. J. Mech. Sci.* **2016**, *113*, 36–48. [CrossRef]
29. Kijima, H. Influence of roll radius on roughness transfer in skin-pass rolling of steel strip. *J. Mater. Process. Technol.* **2014**, *214*, 1111–1119. [CrossRef]
30. Kijima, H. Influence of roll radius on contact condition and material deformation in skin-pass rolling of steel strip. *J. Mater. Process. Technol.* **2013**, *213*, 1764–1771. [CrossRef]
31. Shahani, A.R.; Setayeshi, S.; Nodamaie, S.A.; Asadi, M.A.; Rezaie, S. Prediction of influence parameters on the hot rolling process using finite element method and neural network. *J. Mater. Process. Technol.* **2009**, *209*, 1920–1935. [CrossRef]
32. Yadav, V.; Singh, A.K.; Dixit, U.S. Inverse estimation of thermal parameters and friction coefficient during warm flat rolling process. *Int. J. Mech. Sci.* **2015**, *96–97*, 182–198. [CrossRef]
33. Wang, Z.; Dohda, K.; Haruyama, Y. Effects of entraining velocity of lubricant and sliding velocity on friction behavior in stainless steel sheet rolling. *J. Cent. South Univ.* **2007**, *14*, 224–231. [CrossRef]
34. Zhang, R.Y.; Daymond, M.R.; Holt, R.A. Parametric study of stress state development during twinning using 3D finite element modeling. *Mater. Sci. Eng. A-Struct.* **2011**, *528A*, 2725–2735. [CrossRef]